ACS OMEGA

http://pubs.acs.org/journal/acsodf

Article

Open-Form Configurational Isomers of a Tricyanofuran-Type Metastable-State Photoacid

Juan E. Arias,* David Richardson, Eduardo E. Romero, Mohamed Abdelrahim, Parth K. Patel, Florencio E. Hernandez, and Karin Y. Chumbimuni-Torres*

Cite This: *ACS Omega* 2022, 7, 17538−17543

Read Online

ACCESS | Metrics & More | Article Recommendations | Supporting Information

ABSTRACT: We determine the presence of four open-form configurational isomers for an unsubstituted metastable-state photoacid (mPAH) of the tricyanofuran (TCF) type in solution, at room temperature, via 2D NMR experiments. Electronic structure calculations are carried out to predict the relative stability of the isomers found experimentally and their isomerization barriers. According to the calculated rate constants for isomerization, the molecule can freely interconvert between the open-form isomers, thereby providing a thermal pathway between the isomers that might be better suited to access the cyclized closed-form configuration and those that are not. In establishing the open form isomeric makeup of the TCF mPAH under study, this work establishes the need to consider the four isomers in further studies on the thermal and excited-state isomerization processes and substituent effect thereon.

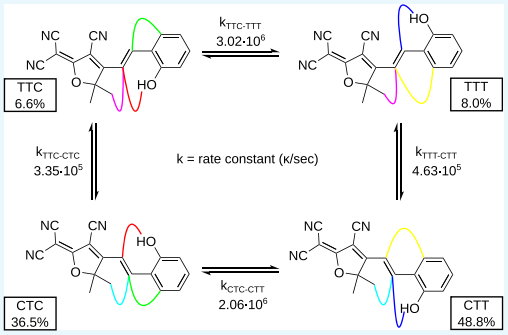

1. INTRODUCTION

Molecular switches provide control over a variety of chemical parameters through external stimuli, such as temperature, light, and pH.[1−3] By providing control over a specific parameter, molecular switches play an important role in diverse applications, such as fluorescence modulation,[4−7] ion detection,[8,9] and polymer functionalization.[10−13] Metastable-state photoacids (mPAHs), first reported in 2011 by Shi et al.,[14] are a family of spiro-style molecular switches capable of reversibly modulating absorbance profiles, polarities, and hydrogen ion concentrations by irradiation with visible light.[15] The colored open form of mPAHs reversibly photocyclisizes into a noncolored, anionic closed form, releasing its hydroxyl proton. Figure 1 illustrates this process for a generic tricyanofuran-type metastable-state photoacid (TCF mPAH),[16] a particular type of mPAH, and makes a contrast with the analogous process in traditional spiro compounds.

The use of mPAHs as molecular switches, as opposed to conventional spiro compounds, like spiropyrans and spirooxazines, has two major advantages. First, photoisomerization is controlled with visible light, as opposed to UV light. As a result, mPAHs are more amenable for use in biological applications and may fare better in regards to photodegradation.[14] Second, mPAHs can modulate pH without the need for prior acidification, as is the case for traditional spiro compounds.[17,18] Prior acidification, like UV light, is a complication for biological applications because it introduces the possibility of damaging the biological environment with the acidifying agent.

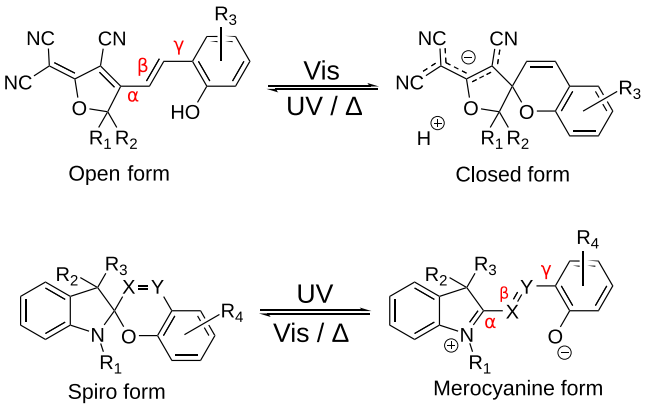

Figure 1. Tricyanofuran-type metastable-state photoacids (top) compared to traditional spiro compounds (bottom).

The potential of TCF mPAHs as molecular switches, particularly in biological applications, warrants the study of their structure and reactivity. Nonetheless, from a mechanistic point of view, the isomerization processes that mPAHs undergo make such studies complex. As with any spiro

Received: November 23, 2021
Accepted: May 6, 2022
Published: May 18, 2022

compound, an understanding of the full picture of the thermal and excited state processes requires the study of both the ground state electronic surface and also excited state surfaces featuring bond breaking and formation and, possibly, conical intersection.[19−21] A labile proton presents, in addition to those of traditional spiro compounds, one additional degree of complexity resulting, all mechanistic features considered, in a formidable challenge to both theory and experiment. As such, any mechanistic study on TCF mPAHs, like those carried out for traditional spiropyrans[19,21−23] and, very recently, for a related merocyanine-type (mer)-mPAH,[24] strongly profits from constraints given by the answer to a simple yet nontrivial question: what configurational isomers are actually present in solution? Experimental evidence on the presence of specific isomers under standard conditions (in other words, at room temperature and in the absence of exciting radiation) informs mechanistic studies by providing the initial structures to be considered in any cyclization pathway, whether it be on an excited or the ground state surface. Given the size and complexity of TCF mPAHs, a number of different configurational isomers arising from bond rotations and the attachment of the labile proton with the different heteroatoms of the molecule, are conceivable. The objective of this paper is to identify the existence of the isomers of an unsubstituted TCF mPHA (R1 = R2 = R3 = H),[16] referred to as TCF1 from here on.

2. RESULTS AND DISCUSSION

The experimental ^{1}H NMR spectra (Table S1 and Figure S1 in the Supporting Information (SI)) reveals seven distinctive signals with clear splitting patterns—six out of the signals integrate to 1. The last one, with a chemical shift of σ_m = 1.77 ppm, and integrating to 6, is the signal coming from the six methyl hydrogens in the molecule. The signals coming from the two vinyl hydrogens (σ_{1v} = 7.42 ppm and σ_{2v} = 8.17 ppm) in the central C═C double bond can be singled out based on their distinctive splitting pattern: they are doublets with a *J*-splitting of 16.4 Hz—a value well within the range for vinyl hydrogens. There is a broad signal at σ = 10.84 ppm likely arising from a strongly deshielded hydrogen. The obvious candidate corresponds to a hydrogen attached to one of the heteroatoms in the molecule and the fact that there is a single signal that integrates to one suggests that only one tautomer is present—Figure S6 in the SI displays the possible locations for the labile proton aside from the phenol hydroxyl group. The remaining four signals can confidently be assigned to the four aromatic hydrogens in the molecule, based on the chemical shielding and splitting patterns. As is the case for phenol,[25,26] it is unlikely that keto−enol tautomerism that places the labile proton in the conjugated carbon atoms, as shown in Figure S6 in the SI, makes a significant contribution to the population for TCF1. Furthermore, such a scenario would be incompatible with the splitting patterns observed experimentally. So far, the ^{1}H NMR is consistent with the general structure proposed for these types of molecules, and the only uncertainty that remains is the location of the labile proton—often presumed to be attached to the phenolic oxygen.

To find experimental evidence for the location of the labile proton, we recorded a ^{13}C NMR spectra and carried out heteronuclear single-quantum coherence (HSQC) and heteronuclear multiple bond correlation (HMBC) experiments—2D NMR experiments that give information about the connectivity of the protons with the carbons in the molecule. The raw

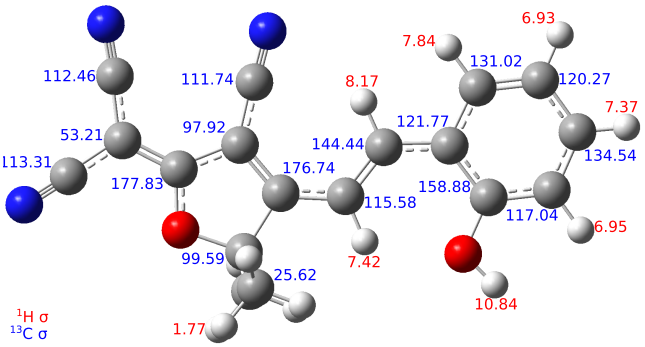

Figure 2. ^{1}H and ^{13}C NMR chemical shifts, as assigned by the HSQC and HMBC experiment.

spectra (Figures S2 and S3 in the SI) and tabulated data (Tables S2 and S3 in the SI) are provided in the SI. On the basis of the information we have about the structure by having made a fraction of the ^{1}H assignments unambiguously, it is possible to use the HSQC and HMBC spectra to assign most of the signals in the ^{13}C NMR. The signals arising from the cyano carbons can still be identified because they are the only closely spaced signals within the range normally associated with cyano carbons, that do not give rise to any HSQC signals. From the HSQC spectra, it is clear that the labile proton is not directly bound to a carbon atom, ruling out the possibility of tautomers where the proton is not attached to a heteroatom in the molecule. No interaction between the methyl hydrogens and the labile proton is present in the HMBC, which rules out the possibility of the proton being attached to the oxygen in the tricyano furan moiety. The HMBC spectra also shows no correlations between the cyano carbons and the labile proton, which rules out the possibility of the proton being attached to the nitrogen atoms in the molecule. The only clear interaction in the HMBC is that of the labile proton with the aromatic carbons, which unambiguously indicates the presence of the tautomer with the proton attached to the phenolic oxygen.

We mention in passing that the presence of the deprotonated open form is ruled out on the basis of UV−vis measurements. The lowest-energy feature in the spectra of mPAHs is red-shifted upon removal of the phenyl hydrogen and prior to cyclization. For example, in the original study on mer-mPAHs, this feature shifts from 424 nm to roughly 550 nm.[14] Only the feature associated with TCF1 with its hydroxyl hydrogen attached, as assigned by predicted UV−vis spectra (Figures S9−S13 in the SI) and in consistency with the original report of the molecule,[16] is observed under the experimental conditions employed throughout the study.

Allowing for rotation about the three C−C bonds that connect the tricyanofuran and phenol moieties (labeled α, β, and γ) in the open form tautomer consistent with the NMR experiments yields a set of eight possible cis−trans configurational isomers. Following standard convention, we denote each of the isomers in question by a label ABC, where A, B, C = T (trans) or C (cis) refers to the configuration about the α, β, and γ bonds, respectively. Spiro compounds are proposed to exist in the cis or, more fittingly, cisoid configuration about the β bond only under forcing conditions[22] or as intermediates in the isomerization between the open and the closed forms.[21,23] The reluctance of spiro compounds to adopt said cis configuration is attributed to the steric hindrance and ensuing nonplanarity of the conjugated system, resulting in a

https://doi.org/10.1021/acsomega.1c06623
ACS Omega 2022, 7, 17538−17543

preferential population of the mostly planar trans configurations. The four TCF1 configurations trans about the β bond are shown in Figure 3.

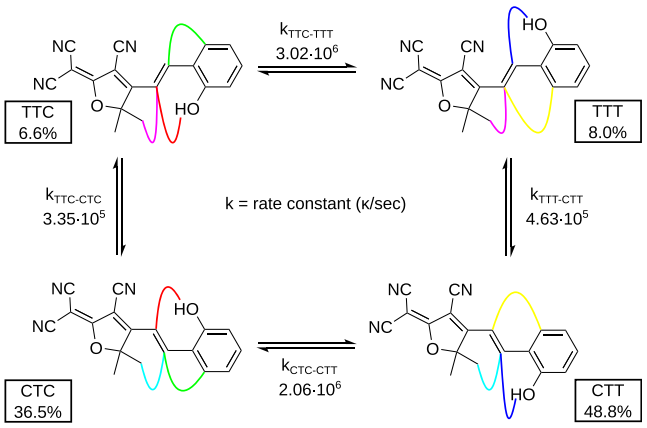

Figure 3. Four open TCF1 isomers with the trans conformation about the β bond, their calculated Boltzmann distribution, and the calculated rate constants of interconversion. The relevant, unique NOE interactions are shown in different colors.

The answer to which configurational isomers of TCF1 should be present is readily addressed by computing a partition function

$$Q = \sum_{\nu} e^{-\beta E_{\nu}} \tag{1}$$

where ν designates a particular configuration of the TCF1 molecule. To obtain the energies required to calculate the partition function we carried out density functional theory (DFT) calculations. We chose a dispersion corrected global hybrid GGA (B3LYP-D3)[27−29] based on Mardirossian and Head-Gordons thorough benchmark, which found it to have a root-mean-squared-deviation of 0.47 kcal/mol in predicting isomerization energies.[30] All calculations were carried out with the Gaussian 09 suite of packages.[31] Figure S7 provides images of the optimized structures; it is clear that they deviate close to nothing from nonplanarity, in contrast to that observed for two mer-mPAHs by Aldaz et al., which feature phenyl and indazole moieties as the donor groups (mer-phenylhydroxy-mPAH and mer-indazole-mPAH, respectively).[24] The distribution resulting from the calculated energies at room temperature (T = 298.25 K) is shown in Figure 3 and Table S5 (SI). DFT predicts the probability of finding a TCF1 molecule in any of the four configuration trans about the β bond

$$P_{\nu} = \frac{e^{-\beta E_{\nu}}}{Q} \tag{2}$$

to be roughly on the same order of magnitude. That is, the ratio P_{ν}/P_{CTT} remains on the order of 10^{-1} for the states ν other than the most stable isomer. This homogeneous distribution, in terms of order of magnitude, differs from calculations carried out for other spiro compounds, where the probabilities of one or two isomers, as calculated by eq 2, dominates over the remaining ($P_{\nu}/P_{\mathrm{moststable}} < 10^{-1}$).[21,23,32] The two isomers with the largest fraction of the population are the CTT and CTC isomers, which is interestingly the opposite of both mer-phenylhydroxy-mPAH and mer-indazole-mPAH, where the predominant isomers are the TTT and TTC.)[24] All the isomers with a cisoid configuration about the β bond were calculated to be too high in energy to make any substantial contribution to the partition function at room temperature (Table S5, SI).

It is clear from Figure 4 that only the cisoid configurations associated with the CTC and the TTC isomers by rotation

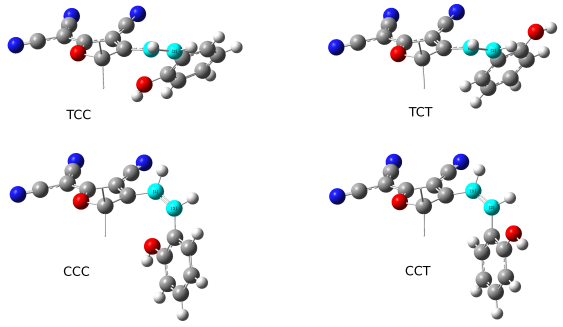

Figure 4. Optimized structures for the four open TCF1 isomers with the cis conformation about the β bond (methyl groups omitted for clarity).

about the β bond, namely, the TCC and CCC isomers, would place the oxygen in the correct position for a nucleophilic attack on the spiro carbon. According to the Boltzmann distribution presented in Figure 3, slightly less than half of the population would be in a configuration that is amenable to cyclization by being one bond rotation away from a cisoid configuration with a direct pathway toward the required nucleophilic attack. If it were the case the CTT and TTT isomers are unable to easily interconvert into either the CTC or TTC isomers by rotations about the γ bond or via a hula twist,[24] it could potentially render a significant fraction of the population unable to reach the closed form, thereby hindering the utility of TCF mPAH as a molecular switch. We note in passing that, in case the CTT and TTT isomers were unable to easily access the CTC and TTC isomers in the ground state, a saving grace for them could be the changes in the different isomerization barriers upon promotion into an excited state surface, removal of the phenolic proton, or both.

To study the possibility of interconversion between the four open form isomers, trans about the β bond, we sought to calculate the reaction rate constants for rotations about the α and γ bonds for each isomer. Transition state theory allows us to compute the rates of rotation k, up to a constant κ (often taken to be 1), by

$$\frac{k}{\kappa} = \frac{k_{\mathrm{B}}T}{h} e^{-\Delta G^{\ddagger}/RT} \tag{3}$$

where the rotational barrier $\Delta G^{\ddagger}$ is defined as the difference in free energy between a transition state and the most stable of the two conformers that it connects. Once again, DFT is able to provide the free energies required to compute $\Delta G^{\ddagger}$. We decided to use the same functional as we used for the isomerization energies, both for consistency and based on the results of the BHROT27 benchmark, which found B3LYP-D3 to have a root-mean-squared deviation of 0.56 kcal/mol in predicting rotational barriers in a variety of organic molecules.[33] The missing geometries (those of the transition states describing the rotation of the α and γ bonds) were obtained via the Synchronous Transit-Guided Quasi-Newton

https://doi.org/10.1021/acsomega.1c06623
ACS Omega 2022, 7, 17538−17543

procedure at the B3LYP-D3/6-311++G(2d, p) level. The free energies of the open form isomers and the transition states were obtained from SPE-calculated energies at the B3LYP/6-311++G(3df, 3pd) level, corrected for entropic contributions at room temperature (T = 298.25 K) calculated at the B3LYP-D3/6-311++G(2d, p) level.

The resulting rate constants at room temperature are shown in Figure 3 and Table S6 (SI). All rate constants are on the order of 10^5−10^6 $(\kappa\ s)^{-1}$. For reference, the rate constants, as calculated by eq 3 based on G2-calculated free energies at room temperature, for the C2−C3 rotation in *n*-butane are 1.12×10^8 for rotations proceeding via the anti−syn (methyl) and the anti−syn (hydrogen) transition states, respectively.[34] We can, therefore, claim that the four open form isomers, trans about the β bond, interconvert between one another via rotations about the α and γ bonds. The α and γ bonds rotate at rates that, although slower than freely rotating alkane bonds by about a factor of 100, are high enough to prevent the TCF1 molecules from getting stuck in one particular isomer, thereby ensuring that even the CTT and TTT isomers are able to access the closed forms through the CTC and TTC isomers. Note that alternative possibility for the CTT and TTT to access the closed form could be to first rotate into their cisoid partners, CCT and TCT, and then rotate about the α bond resulting in the target CCC and TCC isomers or the hula twist that Aldaz et al. reference.[24]

We found three studies providing experimental evidence for the open form isomeric makeup for spironapthooxazines.[35−37] These studies found the TTC and possibly the CTC isomer to be present, in agreement with electronic structure calculations predicting only these isomers to make a substantial contribution to the partition function.[23] In line with these studies and to find experimental evidence for the cis−trans isomers we zoned in on, we carried out a nuclear Overhausser effect (NOE) experiment. The NOE interactions characteristic to each of the four isomers are shown in Figure 3 (the raw spectrum is presented in Figures S4 and S5, SI.) They are those involving interactions between the two vinyl hydrogens in the β bond (σ_{1v} = 7.42 ppm and σ_{2v}= 8.17 ppm) and the methyl hydrogens (σ_m = 1.77 ppm), the aromatic hydrogen ortho to the γ bond (σ_a = 7.84 ppm) and the hydroxyl hydrogen (σ_p = 10.84 ppm.) Note that every unique interaction, denoted with a different color, is present in two isomers.

Table 1 compiles all the information acquired from the NOESY experiment, with the relevant signals color-coded to those depicted in Figure 3. The signal at (σ_{1v}, σ_m) represents an NOE interaction between the methyl hydrogens and the vinyl hydrogen closest to the tricyanofuran core and requires an isomer with the trans configuration about the α bond to be present. However, this is not the only configuration about the α bond implied in this spectra: the signal at (σ_{2v}, σ_m) requires an isomer with the cis configuration about this bond to also be present. In a similar manner, the signals at (σ_{1v}, σ_a) and (σ_{2v}, σ_p) require the presence of an isomer T about the γ bond, and the signals at (σ_{1v}, σ_p) and (σ_{2v}, σ_a) require the presence of an isomer C about the γ bond. At this point, we would like to note that no signal was found at (σ_{1v}, σ_{2v}), representing the absence of an NOE interaction between the vinyl hydrogens. Furthermore, the 16.4 Hz *J*-coupling constant between the vinyl hydrogens lies in the range associated with trans vinyl hydrogens, as opposed to cis vinyl hydrogens. These two observations rule out the presence of the β-cisoid isomers. The three scenarios that can account for the signals observed in the NOE spectra are that (1) the TTC and the CTT isomers are present, (2) the TTT and the CTC isomers are present, and (3) all four isomers are present. In light of our computational work, we believe explanation 3 to be the most plausible. This deviation from the open form isomeric makeup in spironapthooxazines may be due, in part, to the steric hindrance placed by the aromatic hydrogen on the sole hydrogen in the β bond in said molecules. Spiro compounds without the additional aromatic ring in the donor moiety, such as spirooxazines, spiropyrans, and TCF 1, are free of such hindrance.

Table 1. NOE Spectra for TCF1 in DMSO[a]

	10.84	8.17	7.84	7.42	7.37	6.96	6.93	1.77
1.77		●		●				●
6.93			●		●		●	
6.96	●				●	●		
7.37					●	●	●	
7.42	●		●	●				●
7.84		●	●	●			●	
8.17	●	●	●					●
10.84	●	●		●		●		

[a]Both axes correspond to ^{1}H NMR shieldings and relevant NOE signals are color-coded to Figure 3.

3. CONCLUSION

This study provides unambiguous experimental evidence from 1D and 2D NMR experiments for the open form isomeric makeup in solution for TCF 1, in deviance from traditional spiro compounds, to consist of the four configurations trans about the β bond, with the labile hydrogen placed on the phenolic oxygen. The presence of all other prototropy tautomers have been ruled out on the basis of our experimental NMR results. Contributions of the dominant configurations to the population, as computed from density functional theory calculations, appear to be roughly on the same order of magnitude. This could possibly compromise the photochromism of the molecule, since some open forms are unable to access the closed form directly by simple bond rotations. In the present case, TCF 1 circumvents this adversity by a viable pathway for interconversion in between the four configurations at room temperature. A solid understanding of the configurational profile for TCF1 clears the path for further studies on the complicated isomerization processes of this molecule: the thermal ring-closing/opening and the excited-state ring-closing. In a sense, these consist of richer mechanistic problems than those carried out previously for traditional spiro compounds because of the additional degree of complexity imposed by the proton transfer.[24] Progress on the understanding of these complicated isomerization processes will lead to improvements on the design of effective molecular switches.

4. METHODS

Details regarding the synthesis and NMR spectra of TCF can be found in sections 1 and 2 of the SI. For theoretical results, the energies of the eight open form configurations were calculated at the B3LYP-D3/6-311++G(3df,3pd) level, with a

https://doi.org/10.1021/acsomega.1c06623
ACS Omega 2022, 7, 17538−17543

zero point energy (ZPE) correction at the B3LYP-D3/6-311++G(2d,p) level. These energies were calculated from B3LYP-D3/6311++G(2d,p) geometries. Dimethyl sulfoxide (DMSO) was used as the Polarizable Continumm Model (PCM) of solvation (for these and all subsquent calculations) for comparison with experimental NMR results. Additional technical details can be found in section 3 of the SI.

■ ASSOCIATED CONTENT

Supporting Information

The Supporting Information is available free of charge at https://pubs.acs.org/doi/10.1021/acsomega.1c06623.

Synthetic procedure followed to synthesize TCF1, the molecule studied in the main manuscript; raw and tabulated 1D ^{1}H and ^{13}C, HSQC, HMBC, and NOESY NMR data; calculated ground state energies of the configurational isomers studied and the resulting Boltzmann distribution analysis; and (4) theoretical NMR and UV−vis spectra for some of the isomers studied (PDF)

■ AUTHOR INFORMATION

Corresponding Authors

Juan E. Arias − *Department of Chemistry, University of Central Florida, Orlando, Florida 32816, United States;* Present Address: Kenneth S. Pitzer Center for Theoretical Chemistry, Department of Chemistry, University of California, Berkeley, California 94720, USA; Email: juanes@berkeley.edu

Karin Y. Chumbimuni-Torres − *Department of Chemistry, University of Central Florida, Orlando, Florida 32816, United States;* orcid.org/0000-0001-5564-3829; Email: Karin.Y.ChumbimuniTorres@ucf.edu

Authors

David Richardson − *Department of Chemistry, University of Central Florida, Orlando, Florida 32816, United States; Office of Research, University of Central Florida, Orlando, Florida 32816, United States*

Eduardo E. Romero − *Department of Chemistry, University of Central Florida, Orlando, Florida 32816, United States;* Present Address: School of Medicine, University of Colorado, Aurora, CO 80045, USA

Mohamed Abdelrahim − *Department of Chemistry, University of Central Florida, Orlando, Florida 32816, United States*

Parth K. Patel − *Department of Chemistry, University of Central Florida, Orlando, Florida 32816, United States*

Florencio E. Hernandez − *Department of Chemistry, University of Central Florida, Orlando, Florida 32816, United States; The College of Optics and Photonics (CREOL), University of Central Florida, Orlando, Florida 32816, United States*

Complete contact information is available at: https://pubs.acs.org/10.1021/acsomega.1c06623

Notes

The authors declare no competing financial interest.

■ ACKNOWLEDGMENTS

The authors acknowledge the College of Sciences and Department of Chemistry at the University of Central Florida for financial support of this research.

■ REFERENCES

(1) Kathan, M.; Hecht, S. Photoswitchable molecules as key ingredients to drive systems away from the global thermodynamic minimum. *Chem. Soc. Rev.* **2017**, *46*, 5536−5550.

(2) Klajn, R. Spiropyran-based dynamic materials. *Chem. Soc. Rev.* **2014**, *43*, 148−184.

(3) Minkin, V. I. Photo-, Thermo-, Solvato-, and Electrochromic Spiroheterocyclic Compounds. *Chem. Rev.* **2004**, *104*, 2751−2776.

(4) Patel, P. K.; Arias, J. E.; Gongora, R. S.; Hernandez, F. E.; Moncomble, A.; Aloïse, S.; Chumbimuni-Torres, K. Y. Visible light-triggered fluorescence and pH modulation using metastable-state photoacids and BODIPY. *Phys. Chem. Chem. Phys.* **2018**, *20*, 26804−26808.

(5) Yu, Q.; Su, X.; Zhang, T.; Zhang, Y. M.; Li, M.; Liu, Y.; Zhang, S. X. A. Non-invasive fluorescence switch in polymer films based on spiropyran-photoacid modified TPE. *J. Mater. Chem. C* **2018**, *6*, 2113−2122.

(6) Fu, Y.; Han, H. H.; Zhang, J.; He, X. P.; Feringa, B. L.; Tian, H. Photocontrolled Fluorescence "Double-Check" Bioimaging Enabled by a Glycoprobe-Protein Hybrid. *J. Am. Chem. Soc.* **2018**, *140*, 8671−8674.

(7) Zhang, J.; Fu, Y.; Han, H.-H.; Zang, Y.; Li, J.; He, X. P.; Feringa, B. L.; Tian, H. Remote light-controlled intracellular target recognition by photochromic fluorescent glycoprobes. *Nat. Commun.* **2017**, *8*, 987.

(8) Shiraishi, Y.; Nakamura, M.; Hayashi, N.; Hirai, T. Coumarin-spiropyran dyad with a hydrogenated pyran moiety for rapid, selective, and sensitive fluorometric detection of cyanide anion. *Anal. Chem.* **2016**, *88*, 6805−6811.

(9) Patel, P. K.; Chumbimuni-Torres, K. Y. Visible light-induced ion-selective optodes based on a metastable photoacid for cation detection. *Analyst* **2016**, *141*, 85−89.

(10) Connal, L. A.; Franks, G. V.; Qiao, G. G. Photochromic, metal-absorbing honeycomb structures. *Langmuir* **2010**, *26*, 10397−10400.

(11) Bardavid, Y.; Goykhman, I.; Nozaki, D.; Cuniberti, G.; Yitzchaik, S. Dipole assisted photogated switch in spiropyran grafted polyaniline nanowires. *J. Phys. Chem. C* **2011**, *115*, 3123−3128.

(12) Cho, M.-Y.; Kim, J.-S.; Choi, H. J.; Choi, S.-B.; Kim, G.-W. Ultraviolet light-responsive photorheological fluids: as a new class of smart fluids. *Smart Mater. Struct.* **2017**, *26*, 054007.

(13) Yuan, W.; Gao, X.; Pei, E.; Li, Z. Light- and pH-dually responsive dendrimer-star copolymer containing spiropyran groups: synthesis, self-assembly and controlled drug release. *Polym. Chem.* **2018**, *9*, 3651−3661.

(14) Shi, Z.; Peng, P.; Strohecker, D.; Liao, Y. Long-lived photoacid based upon a photochromic reaction. *J. Am. Chem. Soc.* **2011**, *133*, 14699−14703.

(15) Liao, Y. Design and Applications of Metastable-State Photoacids. *Acc. Chem. Res.* **2017**, *50*, 1956−1964.

(16) Yang, C.; Khalil, T.; Liao, Y. Photocontrolled proton transfer in solution and polymers using a novel photoacid with strong C-H acidity. *RSC Adv.* **2016**, *6*, 85420−85426.

(17) Wojtyk, J. T.; Wasey, A.; Xiao, N. N.; Kazmaier, P. M.; Hoz, S.; Yu, C.; Lemieux, R. P.; Buncel, E. Elucidating the mechanisms of acidochromic spiropyran-merocyanine interconversion. *J. Phys. Chem. A* **2007**, *111*, 2511−2516.

(18) Raymo, F. M.; Giordani, S. Signal processing at the molecular level [26]. *J. Am. Chem. Soc.* **2001**, *123*, 4651−4652.

(19) Prager, S.; Burghardt, I.; Dreuw, A. Ultrafast Cspiro-O dissociation via a conical intersection drives spiropyran to merocyanine photoswitching. *J. Phys. Chem. A* **2014**, *118*, 1339−1349.

(20) Savarese, M.; Raucci, U.; Netti, P. A.; Adamo, C.; Rega, N.; Ciofini, I. A qualitative model to identify non-radiative decay

channels: the spiropyran as case study. *Theor. Chem. Acc.* **2016**, *135*, 211.
(21) Liu, F.; Morokuma, K. Multiple pathways for the primary step of the spiropyran photochromic reaction: A CASPT2//CASSCF study. *J. Am. Chem. Soc.* **2013**, *135*, 10693−10702.
(22) Kortekaas, L.; Chen, J.; Jacquemin, D.; Browne, W. R. Proton-Stabilized Photochemically Reversible E/ Z Isomerization of Spiropyrans. *J. Phys. Chem. B* **2018**, *122*, 6423−6430.
(23) Horii, T.; Abe, Y.; Nakao, R. Theoretical quantum chemical study of spironaphthoxazines and their merocyanines: Thermal ring-opening reaction and geometric isomerization. *J. Photochem. Photobiol., A* **2001**, *144*, 119−129.
(24) Aldaz, C. R.; Wiley, T. E.; Miller, N. A.; Abeyrathna, N.; Liao, Y.; Zimmerman, P. M.; Sension, R. J. Experimental and Theoretical Characterization of Ultrafast Water-Soluble Photochromic Photoacids. *J. Phys. Chem. B* **2021**, *125*, 4120−4131.
(25) Capponi, M.; Gut, I.; Wirz, J. The Phenol - 2,4-Cyclohexadienone Equilibrium in Aqueous Solution. *Angew. Chem., Int. Ed. Engl.* **1986**, *25*, 344−345.
(26) Tee, O. S.; Iyengar, N. R. Observation of Transient Cyclohexadienones during the Aqueous Bromination of Phenols. Mechanisms of Enolization. *J. Am. Chem. Soc.* **1985**, *107*, 455−459.
(27) Becke, A. D. A new mixing of Hartree-Fock and local density-functional theories. *J. Chem. Phys.* **1993**, *98*, 1372.
(28) Lee, C.; Yang, W.; Parr, R. G. Development of the Colle-Salvetti correlation-energy formula into a functional of the electron density. *Phys. Rev. B: Condens. Matter Mater. Phys.* **1988**, *37*, 785−789.
(29) Grimme, S.; Antony, J.; Ehrlich, S.; Krieg, H. A consistent and accurate ab initio parametrization of density functional dispersion correction (DFT-D) for the 94 elements H-Pu. *J. Chem. Phys.* **2010**, *132*, 154104.
(30) Mardirossian, N.; Head-Gordon, M. Thirty years of density functional theory in computational chemistry: An overview and extensive assessment of 200 density functionals. *Mol. Phys.* **2017**, *115*, 2315−2372.
(31) Frisch, M. J. et al. *Gaussian 09*, revision E.02; Gaussian, Inc.: Wallingford, CT, 2009.
(32) Maurel, F.; Aubard, J.; Rajzmann, M.; Guglielmetti, R.; Samat, A. A quantum chemical study of the ground state ring opening/closing of photochromic 1,3,3-trimethylspiro[indoline-2,3-naphtho-[2,1-b][1,4]oxazine]. *J. Chem. Soc., Perkin Trans. 2* **2002**, *2*, 1307−1315.
(33) Goerigk, L.; Hansen, A.; Bauer, C.; Ehrlich, S.; Najibi, A.; Grimme, S. A look at the density functional theory zoo with the advanced GMTKN55 database for general main group thermochemistry, kinetics and noncovalent interactions. *Phys. Chem. Chem. Phys.* **2017**, *19*, 32184−32215.
(34) Murcko, M. A.; Castejon, H.; Wiberg, K. B. Carbon-carbon rotational barriers in butane, 1-butene, and 1,3-butadiene. *J. Phys. Chem.* **1996**, *100*, 16162−16168.
(35) Nakamura, S.; Uchida, K.; Murakami, A.; Irie, M. Ab initio MO and proton NMR NOE studies of photochromic spironaphthoxazine. *J. Org. Chem.* **1993**, *58*, 5543−5545.
(36) Delbaere, S.; Luccioni-Houze, B.; Bochu, C.; Teral, Y.; Campredon, M.; Vermeersch, G. Kinetic and structural studies of the photochromic process of 3H-naphthopyrans by UV and NMR spectroscopy. *J. Chem. Soc., Perkin Trans. 2* **1998**, *2*, 1153−1158.
(37) Laréginie, P.; Lokshin, V.; Samat, A.; Guglielmetti, R.; Pèpe, G. First permanent opened forms in spiro[indoline-oxazine] series: synthesis and structural elucidation. *J. Chem. Soc., Perkin Trans. 2* **1996**, *1*, 107−111.

https://doi.org/10.1021/acsomega.1c06623
ACS Omega 2022, 7, 17538−17543